Chitosan/Carboxymethyl Cellulose Nanocomposites Prepared via Electrolyte Gelation–Spray Drying for Controlled Ampicillin Delivery and Enhanced Antibacterial Activity

Anh Dzung Nguyen *, Vinh Nghi Nguyen, Vu Hoa Tran, Huu Hung Ding, Dinh Sy Nguyen, Thi Huyen Nguyen, Van Bon Nguyen, San-Lang Wang *

Posted Date: 1 January 2026

doi: 10.20944/preprints202512.2817.v1

Keywords: chitosan; carboxymethyl cellulose; nanocomposite; ampicillin; spray drying; antibacterial activity

 doi:10.20944/preprints202512.2817.v1

Article

Chitosan/Carboxymethyl Cellulose Nanocomposites Prepared via Electrolyte Gelation–Spray Drying for Controlled Ampicillin Delivery and Enhanced Antibacterial Activity

Anh Dzung Nguyen [1,*], Vinh Nghi Nguyen [2], Vu Hoa Tran [1], Huu Hung Ding [3], Dinh Sy Nguyen [1], Thi Huyen Nguyen [1], Van Bon Nguyen [1] and San-Lang Wang [4,*]

[1] Institute of Biotechnology and Environment, Tay Nguyen University, Buon Ma Thuot 630000, Vietnam
[2] Ninh Thuân Hospital, Khanh Hoa, 650000, Vietnam
[3] Faculty of Medicine and Pharmacy, Tay Nguyen University, Buon Ma Thuot 630000, Vietnam
[4] Department of Chemistry, Tamkang University, New Taipei, Taiwan
* Correspondence: nadzung@ttn.edu.vn (A.D.N.); sabulo@mail.tku.edu.tw (S.-L.W.)

Abstract

This study reports the fabrication of chitosan/carboxymethyl cellulose (C/M) nanocomposites by electrolyte gelation-spray drying and the evaluation of their antibacterial performance as carriers for the antibiotic ampicillin. Chitosan (C), a cationic biopolymer derived from chitin, was combined with the anionic polysaccharide carboxymethyl cellulose (M) at different mass ratios to form stable nanocomposites via electrostatic interactions and then collected by a spraying dryer. The resulting particles exhibited mean diameters ranging from 800 to 1500 nm and zeta potentials varying from +90 to −40 mV, depending on the C:M ratio. The optimal formulation (C:M = 2:1 ratio) achieved a high recovery yield (71.1%) and ampicillin encapsulation efficiency EE (82.4%). Fourier transform infrared spectroscopy (FTIR) confirmed the presence of hydrogen bonding and ionic interactions among C:M, and ampicillin within the nanocomposite matrix. The nano-microcomposites demonstrated controlled ampicillin release and pronounced antibacterial activity against *Staphylococcus aureus*, with minimum inhibitory concentration (MIC) and minimum bactericidal concentration (MBC) values of 3.2 μg/mL and 5.3 μg/mL, respectively, which were lower than those of free ampicillin. These results indicate that the chitosan/carboxymethyl cellulose nano-microcomposites are promising, eco-friendly carriers for antibiotic delivery and antibacterial applications.

Keywords: chitosan; carboxymethyl cellulose; nanocomposite; ampicillin; spray drying; antibacterial activity

1. Introduction

Chitosan, a derivative of chitin, is a linear natural polymer widely distributed in the shells of crustaceans, insects, and fungal cell walls. Due to its natural origin, biocompatibility, biodegradability, and low toxicity, chitosan has been extensively investigated as a promising material for drug delivery systems. As a naturally occurring polycation (poly-NH_4^+), chitosan readily interacts with negatively charged biological membranes and biomolecules, facilitating drug encapsulation and cellular uptake [1,2].

At the nanoscale, nanochitosan offers several advantages for drug delivery applications, including high surface area, tunable surface charge, and improved interaction with biological barriers. In addition to its intrinsic antibacterial activity, nanochitosan can enhance drug bioavailability by improving drug stability, prolonging residence time, and enabling controlled or sustained drug release. The interaction between positively charged nanochitosan and negatively

 doi:10.20944/preprints202512.2817.v1

charged bacterial membranes or nucleic acids further contributes to the synergistic antibacterial efficacy of drug-loaded systems [3,4].

Nanochitosan has been widely employed as a carrier for various antibiotics, such as ampicillin, amoxicillin, ciprofloxacin, chlortetracycline, and gentamicin, with the aim of enhancing antibacterial efficacy and overcoming antibiotic resistance [5–8]. Nevertheless, several limitations hinder its practical application in drug delivery, including high production costs, insufficient particle stability under acidic conditions, and relatively low drug loading and release efficiency associated with the linear molecular structure of chitosan. Moreover, many conventional nanochitosan fabrication methods—except spray drying—suffer from low recovery yields and the use of undesirable chemical reagents, which restrict their scalability and biomedical applicability [9].

Cellulose, similar to chitosan, are natural, biocompatible, and biodegradable polymers that have also been explored as drug carriers in the form of nanoparticles, nanofilms, and nanofibers. However, drug delivery systems based solely on starch or cellulose often exhibit poor mechanical properties, limited structural stability, and rapid enzymatic degradation, leading to uncontrolled drug release and reduced therapeutic efficiency [10,11]

Therefore, to improve drug loading capacity, structural stability, and release performance while reducing production costs, chitosan can be combined with negatively charged polymers such as alginate, cellulose, and starch to form nanocomposite or multilayered drug delivery systems via electrostatic interactions. These nanocomposites provide enhanced network structures, improved physicochemical stability, and greater control over drug encapsulation and release, making them highly promising platforms for advanced drug delivery applications [12–15].

limitations remain, including poor structural stability, limited drug loading capacity, and uncontrolled release resulting from the linear molecular structure of chitosan. In addition, many reported fabrication methods involve complex processes, low recovery yields, or the use of chemical crosslinkers, which restrict scalability and biomedical applicability. Comparative investigations on the effects of polymer composition and molecular weight on drug delivery performance, particularly for nanocomposite systems produced by scalable techniques such as spray drying, are still limited. Therefore, this study aims to develop chitosan-based nanocomposite drug delivery systems by combining chitosan with natural polysaccharides, including carboxymethyl cellulose, to improve drug loading efficiency, structural stability, and controlled release behavior. The findings are expected to contribute to the rational design of efficient and cost-effective polysaccharide-based nanocarriers for drug delivery applications.

2. Materials and Methods

Materials

Chitosan (Sigma, USA; Mw ≈ 500 kDa, degree of deacetylation >75%, purity >95%) was used as the primary polymer. Sodium carboxymethyl cellulose (CMC) and sodium tripolyphosphate (TPP) were obtained from Merck (Germany). Ampicillin sulfate was purchased from Sigma-Aldrich (USA). Nutrient Broth was supplied by Himedia (India). Antimicrobial-resistant *Staphylococcus aureus* ATCC 25923 was provided by the Pasteur Institute, Ho Chi Minh City, Vietnam

Preparation of Ampicillin-Loaded Chitosan/CMC Nanocomposites

Chitosan (0.1% w/v) was dissolved in 0.1 N acetic acid, while CMC (0.1% w/v) was prepared in deionized water. Ampicillin was incorporated into the chitosan/CMC mixtures to obtain final concentrations ranging from 0 to 7.5 μg/mL. Chitosan (C) and CMC (M) were mixed at different weight ratios and magnetically stirred for 60 min at room temperature.

Nanocomposite particles were spontaneously formed via ionic gelation between positively charged chitosan and negatively charged CMC. The suspensions were spray-dried using a nano spray dryer (B-90, Büchi, Switzerland) under optimized conditions: inlet temperature 120 °C, outlet

 doi:10.20944/preprints202512.2817.v1

temperature 80 °C, feed rate 120 mL/h, compressed air flow 1.2 m^3/min, and nozzle diameter 5.5 μm [16]. All formulations were prepared in triplicate.

Characterization of Nanocomposites

Particle morphology and elemental composition were examined using SEM–EDS (Phenom ProX, Thermo Scientific, USA). Mean particle size, size distribution, and zeta potential were measured using a Nanosizer SZ-100 (Horiba, Japan) at 25 °C. Chemical interactions between chitosan, ampicillin, and CMC were analyzed by FT-IR spectroscopy (Alpha, Bruker, USA) in the range of 500–4000 cm^{-1}.

Ampicillin Encapsulation Efficiency and Release Kinetics

Encapsulation efficiency (EE %) and release behavior of ampicillin were determined using a centrifugation-based method adapted from Schumacher (1997) [17]. Briefly, 50 μg of nanocomposite was dispersed in PBS (pH 7.0) and centrifuged at 14,000 rpm at 5 °C. The supernatant containing free ampicillin was quantified, while the pellet was resuspended in fresh PBS for release studies conducted over 24 h at room temperature.

Ampicillin concentration was quantified by HPLC (UHPLC Thermo 3000) equipped with a Hypersil GOLD PFP column using MeOH/ACN/HCOOH (30:40:30, v/v/v) as the mobile phase at a flow rate of 0.2 mL/min and detection wavelength of 270 nm. Encapsulation efficiency was calculated as:

$$LE\ (\%) = \frac{(Qt - Qs) \times 100}{Qt}$$

where Q_t is the total initial amount of ampicillin and Q_s is the amount of non-encapsulated ampicillin.

Antibacterial Activity Assay

Antibacterial activity was evaluated against *S. aureus* (10^6 CFU/mL) cultured in Nutrient Broth containing ampicillin-loaded chitosan/CMC nanocomposites (0–7.5 μg/mL). Cultures were incubated at 37 °C for 48 h with shaking at 120 rpm. Bacterial growth was monitored by measuring optical density at 620 nm using a UV-Vis spectrophotometer (Jasco, Japan). Antibacterial efficacy was expressed as inhibition efficiency (I%) [18].

$$I\ (\%) = (B-K)/B*100\%$$

In which: The inhibiton eficiency (I%). B: average OD620 index of the control. K: Average OD620 index of chitosan/CMC nanocomposite loaded ampicillin.

Determination of MIC and MBC

Minimum inhibitory concentration (MIC) was determined using the broth dilution–resazurin method, while minimum bactericidal concentration (MBC) was assessed by agar diffusion. MIC and MBC values were defined as the lowest concentrations preventing visible bacterial growth after incubation at 37 °C for 24 h.

Statistical Analysis

All experiments were performed in triplicate. Data were analyzed using one-way ANOVA followed by Duncan's multiple range test ($p < 0.05$) with SPSS 20.0. Results are presented as mean ± standard deviation (SD).

3. Results and Discussion

 doi:10.20944/preprints202512.2817.v1

3.1. Effect of Chitosan/Carboxymethyl Cellulose Ratio on the Properties of Chitosan/Cellulose Nanocomposites Prepared by Spray Drying

The interplay between chitosan and carboxymethyl cellulose (CMC) in polyelectrolyte complexes critically determines the physicochemical properties of the resulting composite particles. Chitosan, a cationic polysaccharide, interacts electrostatically with the anionic carboxylate groups of CMC, leading to complexation that strongly influences particle size, surface charge, and stability upon spray drying. Such ionic interactions have been increasingly investigated for tailored nanocomposite materials with enhanced functional properties [19].

3.1.1. Particle Size and Morphology

As summarized in Table 1, the mean particle diameter of chitosan/CMC nanocomposites varied systematically with composition. Pure chitosan (C100) formed relatively small particles (~816 nm), whereas increasing CMC content led to progressively larger particles — reaching approximately 1500 nm at the highest CMC ratio (C1M5). This trend reflects the increased prevalence of ionic crosslinks and the concomitant formation of dense polyelectrolyte complexes that aggregate into larger clusters prior to spray drying. The gradual increase in particle size with higher CMC content suggests stronger electrostatic interactions and complexation kinetics that favor the formation of larger precursors before atomization and solvent removal. These observations align with recent work demonstrating the importance of polyelectrolyte balance on particle formation mechanisms in spray-dried systems [12,19].

Table 1. Effect of Chitosan/Carboxymethyl Cellulose Ratio on the Properties of Chitosan/Cellulose Nanocomposites Prepared by Spray Drying.

No	Samples	Chitosan/CMC ratio (w/w)	Zeta potential (mV)	Mean particle size (nm)	Yield (%)	Loading efficiency of ampicillin (%)
1	C100	1:0	67.67±0.92	816.9±24.5^{e}	75.49±0.35^{a}	68.6±1.2^{c}
2	C5M1	5:1	82.70±0.45	954.2±20.3^{e}	72.03±0.06^{b}	78.8±0.9^{b}
3	C4M1	4:1	85.07±1.81	1049.8±28.7^{d}	71.88±0.07^{b}	79.2±1.3^{b}
4	C3M1	3:1	89.53±1.89	1144.4±32.0^{d}	71.17±0.04^{b}	81.8±0.7^{a}
5	C2M1	2:1	90.37±1.05	1288.8±24.3^{c}	71.08±0.03^{b}	82.4±1.4^{a}
6	C1M1	1:1	78.63±1.02	1290.4±35.0^{c}	71.04±0.05^{b}	80.1±0.9^{b}
7	C1M2	1:2	61.67±2.45	1304.7±26.3^{c}	70.71±0.06^{c}	75.8±1.9^{c}
8	C1M3	1:3	-31.43±0.65	1313.0±18.2^{c}	69.15±0.03^{d}	58.6±0.7^{d}
9	C1M4	1:4	-39.17±0.05	1652.5±42.5^{b}	69.06±0.04^{d}	56.3±0.4^{d}
10	C1M5	1:5	-40.00±0.72	1906.8±40.4^{a}	68.72±0.60^{e}	50.8±0.8^{e}
11	M100	0:1	-81.73±0.90	1658.9±38.7^{b}	67.01±0.06^{e}	38.8±0.6^{f}

**Values are presented as mean ± standard deviation (n = 3). Different superscript letters (a–f) within the same column indicate statistically significant differences (p < 0.05).*

In contrast to our findings with CMC, reported studies on other chitosan-based composites indicate differing particle size behavior depending on the complementary polymer and processing method. For example, chitosan nanoparticles prepared by ionic gelation with tripolyphosphate exhibited size and surface charge variations dependent on polymer ratios and process conditions, highlighting how crosslinker type and electrostatic balance modulate final morphology [20–22].

3.1.2. Zeta Potential and Colloidal Stability

Zeta potential measurements further elucidated the impact of polymer ratio on surface charge. The size distribution of all samples was ranged from 100-1900 nm. As shown in Table 1 and Figure 3, decreasing chitosan fraction systematically reduced the net positive surface charge due to the increasing contribution of negatively charged CMC. High absolute zeta potentials (> |30| mV) are

 doi:10.20944/preprints202512.2817.v1

generally associated with improved colloidal stability by electrostatic repulsion, which is consistent with the strong charge interactions observed in our chitosan/CMC complexes.

Recent literature on spray-dried chitosan microparticles corroborates the critical role of charge balance and processing conditions on zeta potential and stability. Specifically, reviews of inhalable chitosan-based spray-dried composites report that both formulation parameters and drying techniques significantly influence charge distribution, particle aggregation, and aerodynamic performance of chitosan-containing particles [16,19].

The distinct particle size behavior observed in our chitosan/CMC system — increasing with higher CMC content — contrasts with reports where increasing content of other polysaccharides (e.g., starch) resulted in decreasing particle sizes in chitosan composites. This discrepancy underscores the importance of the interacting polymer's intrinsic charge density and molecular architecture on complexation dynamics and spray drying outcomes [21,22].

More broadly, recent advances in polyelectrolyte-complexed biopolymer particles continue to highlight how subtle differences in polymer charge density, molecular weight, and processing parameters can dramatically alter morphology, surface charge, and functionality. For example, chitosan/CMC systems with incorporated functional nanoparticles (e.g., silver) have been shown to yield enhanced antimicrobial and hemostatic properties, further illustrating how tailored composition can tune both physical and biological performance [12].

Understanding the relationship between polymer ratio, complexation behavior, and the resulting physicochemical properties is essential for designing functional nanocomposites for applications such as drug delivery, hemostatic materials, and environmentally responsive carriers. The ability to tune particle size and surface charge via simple formulation adjustments provides a versatile platform for exploiting chitosan/CMC interactions in diverse contexts.

The antibacterial activity of chitosan is closely related to its positive surface charge, as reflected by the zeta potential. As shown in Table 1, spray-dried chitosan nanoparticles (C100) obtained in this study exhibited a high zeta potential of +67.67 mV, which is markedly higher than values reported in previous studies (+30 to +55 mV) for chitosan nanoparticles prepared by spray drying or ionic gelation–spray drying combinations [16,19,21,22].

Earlier reports showed that chitosan nanoparticles prepared using sodium tripolyphosphate (TPP) typically possess much lower zeta potentials (+25 to +29 mV), while crosslinked and spray-dried chitosan nanoparticles exhibited values below +35 mV. These comparisons indicate that the fabrication strategy employed in the present work enables the generation of chitosan nanoparticles with unusually high surface charge [16,19].

For chitosan/cellulose nanocomposites, the zeta potential increased significantly with changes in the chitosan-to-CMC ratio, reaching +78.63 mV (C1M1), +85.07 mV (C4M1), +89.53 mV (C3M1), and a maximum of +90.37 mV (C2M1). This enhancement is attributed to strong ionic interactions between positively charged chitosan and negatively charged carboxymethyl cellulose (CMC), promoting the formation of electrostatically stabilized nano- and microcomposite particles.

A core–shell-like structure is proposed, in which CMC-rich domains form the particle core, while chitosan chains are preferentially enriched at the particle surface, resulting in a high density of positive charges. This structural arrangement is supported by FT-IR analysis (Figure 4) and is consistent with observations for chitosan/carboxymethyl cellulose nanocomposites (Table 1), although the magnitude of the zeta potential enhancement is more pronounced in the chitosan/carboxymethyl cellulose system.

When the CMC content exceeded 50%, the zeta potential decreased sharply to +61.67 mV (C1M2) and further to negative values (−31.43 to −40.00 mV for C1M3–C1M5). This behavior is explained by the intrinsically high negative surface charge of CMC (−81.73 mV), which dominates the composite surface at high cellulose fractions. In contrast, starch exhibits a much lower negative zeta potential, leading to different charge evolution trends in chitosan/starch nanocomposites [21,22].

These findings are consistent with recent studies showing that polymer charge density and composition strongly influence zeta potential and surface properties. Some works reported a

 doi:10.20944/preprints202512.2817.v1

significant reduction in absolute zeta potential upon polymer modification and drug loading, highlighting the sensitivity of surface charge to compositional changes [23,24]

Overall, the combined results from Tables 1 and Figure 1, Figure 2 and Figure 3 demonstrate that chitosan-based nanocomposites formulated with appropriate cellulose or starch ratios can achieve exceptionally high zeta potentials (+70 to +90 mV), exceeding those of pristine chitosan nanoparticles and most literature reports (+20 to +50 mV). This enhanced surface charge is likely associated with a two-layered nanostructure, which may contribute to improved colloidal stability and antibacterial performance.

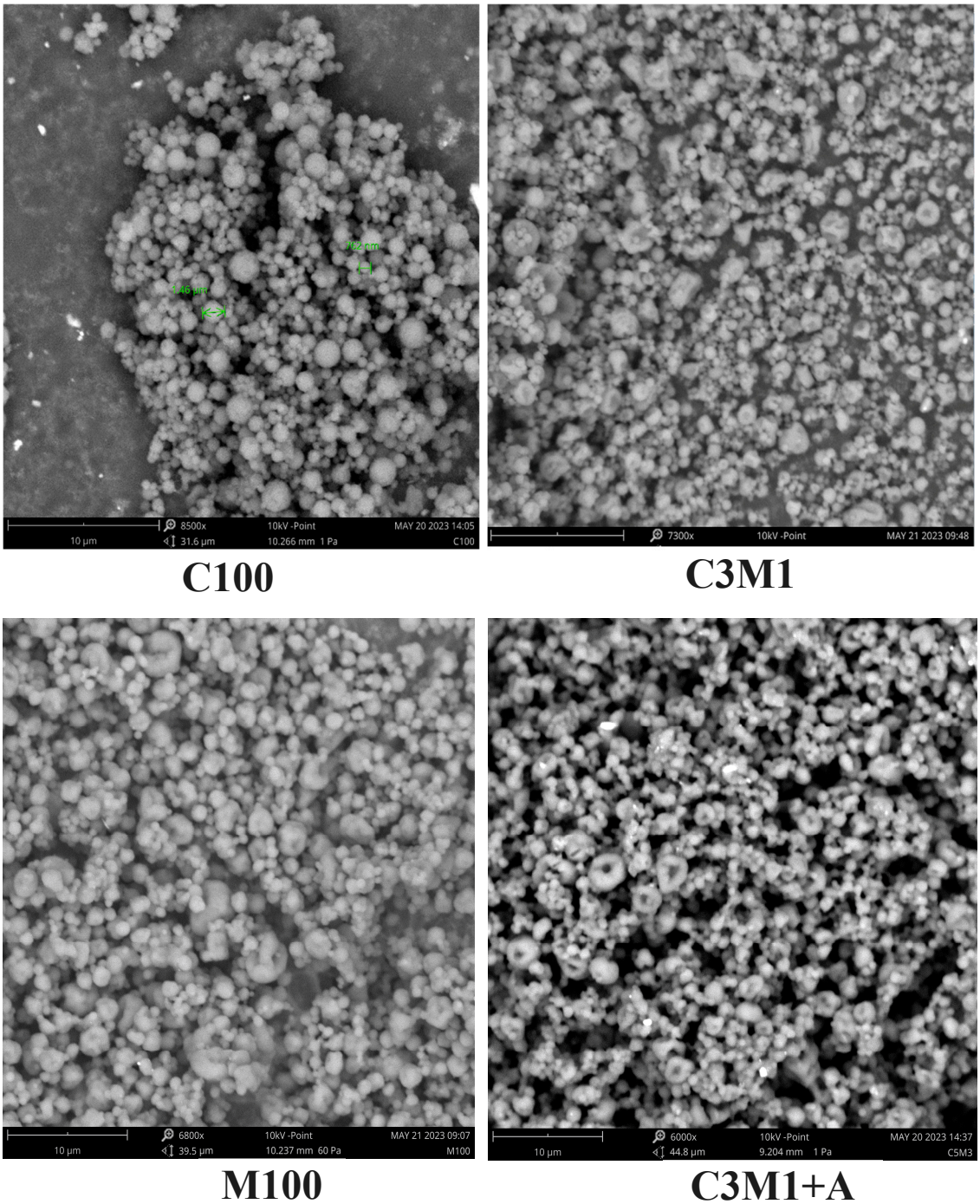

Figure 1. SEM images of chitosan/carboxymethyl cellulose nanocomposite and nano chitosan/carboxymethylcellulose composite loaded ampicilline. (Taken by SEM, Phenome ProX, Thermo, USA; 8000x, 10kV, bar 10 um).

 doi:10.20944/preprints202512.2817.v1

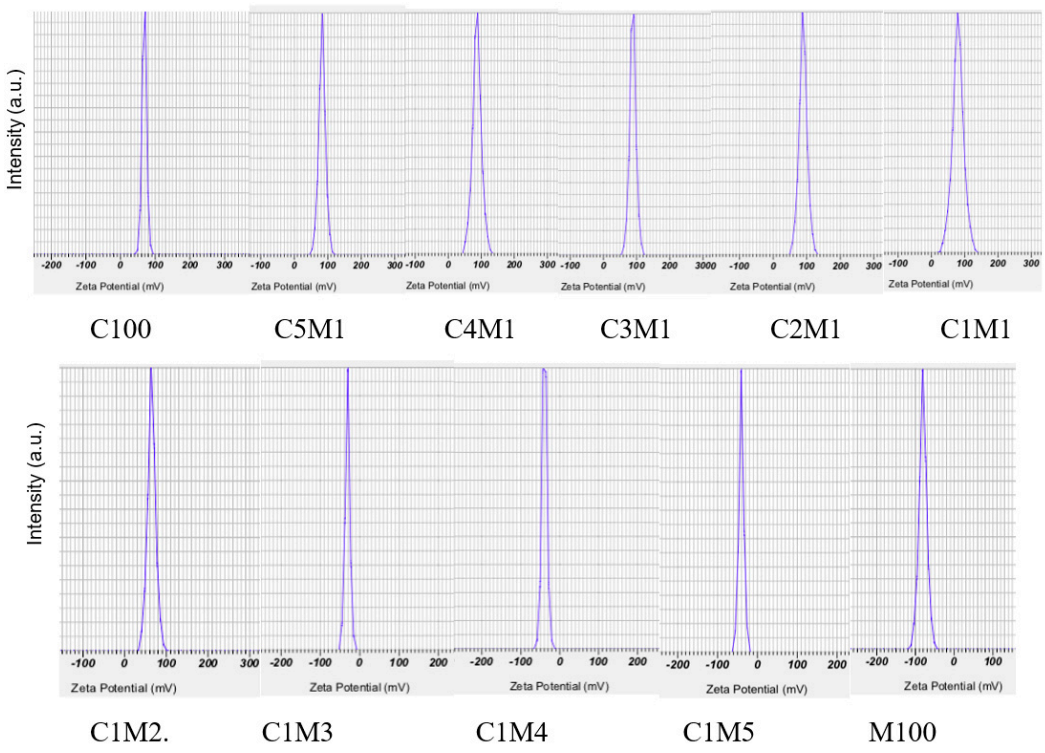

Figure 2. Effect of chitosan/carboxymethyl cellulose ratio on the the zeta potential of the nanocomposite (Analysed by a Nanosizer SZ 100, Horiba, Japan, at 25^{0}C).

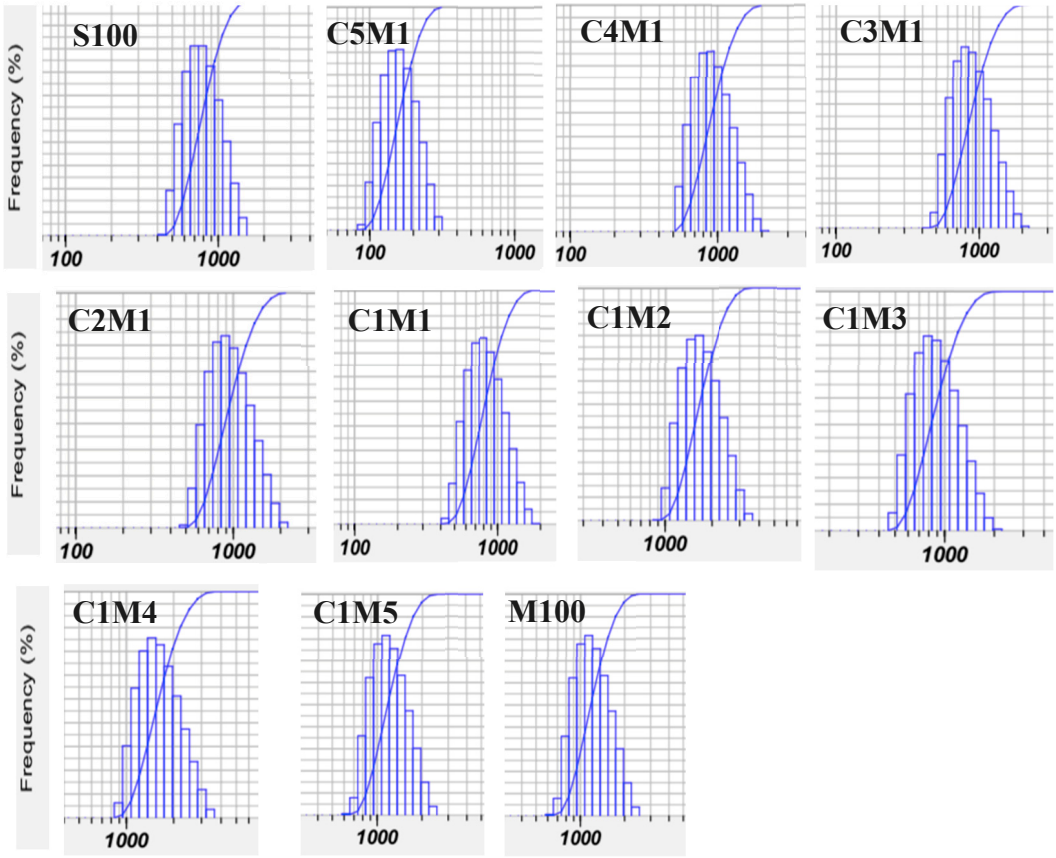

Figure 3. Effect of chitosan/carboxymethyl cellulose ratio on the size distribution of the nanocomposite (Analysed by a Nanosizer SZ 100, Horiba, Japan, at 25^{0}C).

 doi:10.20944/preprints202512.2817.v1

3.1.3. Particle Size Distribution and Recovery Yield

Figure 3, Table 1 illustrates that the chitosan/carboxymethyl cellulose ratio strongly affects particle size distribution. Compared with earlier studies reporting broad size distributions (1–8 μm) and low zeta potentials, the present system exhibits improved charge characteristics and more controlled particle formation [25].

Spray drying afforded high recovery yields ranging from 67.01% to 75.49%, with composite formulations achieving yields of approximately 70–72%. These values are comparable to chitosan/starch nanocomposites and significantly higher than yields reported in previous studies (47–62%), confirming the efficiency of combining ionic complexation with spray drying for the production of chitosan-based nanocomposites [21,22].

3.1.4. FT-IR Analysis of Chitosan/Carboxymethyl Cellulose Nanocomposites

The FT-IR spectrum of ampicillin (Amp) (Figure 4f) shows characteristic absorption bands at ~3444 cm^{-1}, attributed to N–H stretching of amine and amide groups and O–H stretching of carboxylic groups. Bands around 2900 cm^{-1} correspond to C–H stretching vibrations, while the most distinctive peak at 1765 cm^{-1} is assigned to C=O stretching of the β-lactam ring. Additional bands between 1660 and 1599 cm^{-1} are related to N–H bending of primary amine groups [26,27]

The FT-IR spectrum of carboxymethyl cellulose (CMC, M100) (Figure 4b) exhibits typical bands at ~3450 cm^{-1} (O–H stretching), 2927 cm^{-1} (C–H stretching), and 1064 cm^{-1} (C–O–C stretching of glycosidic bonds). The absorption near 1636 cm^{-1} is associated with carboxylate ($–COO^-$) groups. Similarly, chitosan (C100) (Figure 5c) displays characteristic bands at ~3449 cm^{-1} (overlapping O–H and $–NH_2$ stretching), ~2930 cm^{-1} (C–H stretching), ~1641 cm^{-1} (N–H bending), and ~1064 cm^{-1} (C–O–C stretching) [28,29]

The FT-IR spectrum of ampicillin-loaded chitosan/cellulose nanocomposites (C2M1+Amp) (Figure 4d) contains the main characteristic bands of all components, confirming successful incorporation of ampicillin into the composite matrix. Broad absorption around 3450 cm^{-1} and bands near 2900 cm^{-1} arise from overlapping functional groups of Amp, CMC, and chitosan. Importantly, the β-lactam C=O band at 1765 cm^{-1} remains detectable, indicating that the chemical structure of ampicillin is preserved after encapsulation.

Notably, the N–H bending bands of ampicillin at 1660 and 1599 cm^{-1} shift slightly to ~1653 and ~1596 cm^{-1} in the nanocomposite, providing evidence for hydrogen bonding and/or ionic interactions between ampicillin and functional groups of the composite, particularly hydroxyl groups of CMC and protonated amino groups ($–NH_3^+$) of chitosan [30,31].

Overall, the FT-IR results confirm the formation of a network-like chitosan/carboxymethyl cellulose nanocomposite stabilized by ionic interactions and hydrogen bonding. These interactions contribute to structural stability and are expected to retard ampicillin release from the particles. Combined with zeta potential data, the FT-IR analysis supports a core–shell-like structure, in which negatively charged CMC forms the core, while positively charged chitosan is enriched at the particle surface. Ampicillin is preferentially associated with the chitosan-rich outer layer through electrostatic and hydrogen-bonding interactions, explaining the high zeta potential and improved stability observed at optimal chitosan/CMC ratios.

 doi:10.20944/preprints202512.2817.v1

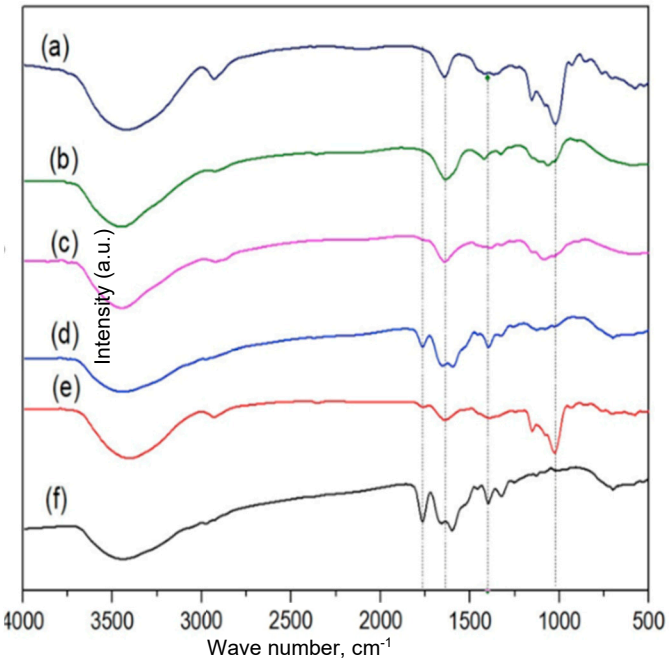

Figure 4. FT-IR of chitosan/carboxymethyl cellulose nanocomposite. S100 (a): starch; M100 (b); C100 (c); C2M1+Amp (d); C1S2+Amp (e) và Amp (f). (FTIR Alpha, Brucker, USA) with a range of 500-4000 cm^{-1} at a resolution of 16 cm^{-1} within 32 scans).

3.1.5. The Release Profile of Ampicillin from Chitosan/Carboxymethyl Cellulose Nanocomposite

The release profiles (Figure 5) show a typical biphasic behavior, consisting of an initial burst release followed by a slower, sustained-release phase. During the early period (≈0–1 h), all formulations exhibit a rapid increase in cumulative drug release, indicating that a fraction of the drug is likely adsorbed/weakly bound at or near the particle surface and is therefore released quickly upon contact with the medium. After this initial stage, the release rate decreases markedly and becomes more gradual from ≈2 h onward, suggesting that drug transport is increasingly governed by diffusion through the polymeric matrix and/or swelling–relaxation of the polymer network **(**Korsmeyer–Peppas**,** diffusion vs swelling/relaxation) [21,22].

Notably, the cumulative release approaches a plateau (~70% for the nanocomposite, and 75% for chitosan nanoparticles at 24 h) for most samples, implying that a portion of the drug may remain more strongly entrapped within the matrix or associated with less-accessible domains, which is consistent with a controlled, prolonged release system rather than immediate release. Overall, the sustained phase and the late-time plateau support the conclusion that the carrier system provides release retardation, potentially reducing dosing frequency and maintaining therapeutic levels over an extended period.

 doi:10.20944/preprints202512.2817.v1

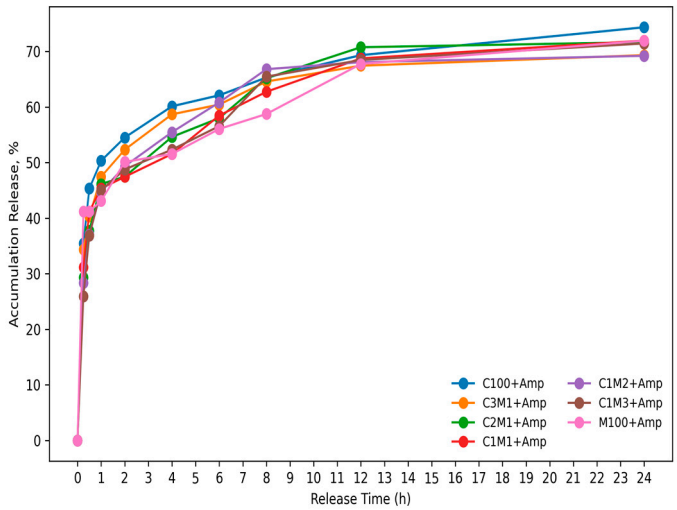

Figure 5. Release profiles of ampicillin from chitosan/carboxymethyl cellulose nanocomposite. Ampicillin concentration of 7.5 µg/mL, in phosphate buffer solution (PBS), pH=7.0 within 24h; values in the figure are mean of triplicates ± SE).

3.2. Antibacterial Activity of Ampicillin-Loaded Chitosan/Cellulose Nanocomposites Against Staphylococcus aureus

Staphylococcus aureus is a major opportunistic pathogen commonly colonizing the skin and upper respiratory tract and is responsible for a wide range of infections, particularly in immunocompromised individuals. The rapid emergence of multidrug-resistant *S. aureus*, especially MRSA strains, has significantly reduced the clinical efficacy of conventional β-lactam antibiotics, including ampicillin. Therefore, nano-enabled antibiotic delivery systems that protect antibiotics from enzymatic degradation and enhance antibacterial efficacy represent a promising therapeutic strategy [32].

3.2.1. Effect of Ampicillin Loading on Antibacterial Activity

Ampicillin-loaded chitosan/cellulose nano- and microcomposites were prepared with initial ampicillin concentrations ranging from 0 to 7.5 µg/mL prior to spray drying. As summarized in Table 1 pristine chitosan nanoparticles (C100) exhibited an encapsulation efficiency (EE) of 68.6%, comparable to that of chitosan/starch nanocomposites. In contrast, chitosan/cellulose nanocomposites showed significantly higher EE values, reaching 78.8% (C5M1), 81.8% (C3M1), and 82.4% (C2M1), exceeding those reported for chitosan/starch systems (60–77%) [21,22]. Other works reported that cephalosporin antibiotics and β-lactamase inhibitors were loaded into chitosan nanoparticles or ampicilline in chitosan/starch nanocomposite (60-65%). The encapsulation efficiency of cefotaxime and ceftiofur was approximately 70% and 60%, lower than those this study. Ampicillin was encapsulated in the liposome; however, the reported encapsulation efficiency of ampicillin was 50%, which is lower than the efficiency observed in this study [17,21,22,33].

The enhanced encapsulation efficiency is attributed to the formation of a dense ionic network between positively charged chitosan (+67 mV) and highly negatively charged carboxymethyl cellulose (−81 mV). This network retains ampicillin, which carries a net negative charge, within the composite matrix while maintaining a high positive surface charge (+70 to +90 mV). However, further increasing the cellulose fraction resulted in a gradual decrease in EE (75.8% for C1M2, 58.6% for C1M3, and 50.8% for C1M5). Pure CMC nanoparticles (M100) exhibited the lowest EE (≈38%), due to electrostatic repulsion between negatively charged CMC and ampicillin and the absence of a network structure.

 doi:10.20944/preprints202512.2817.v1

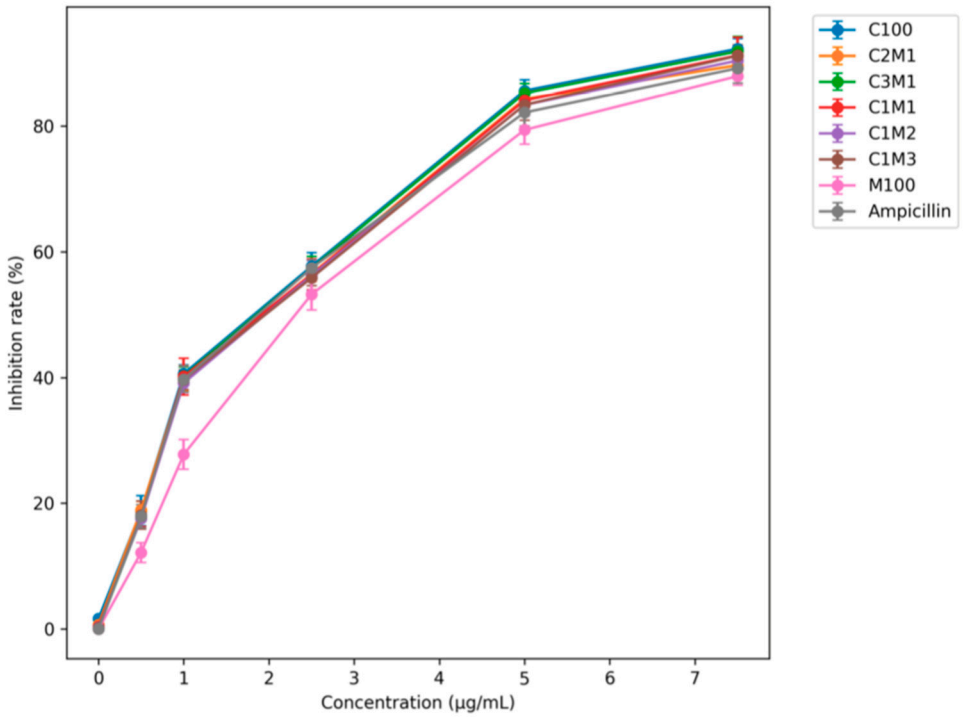

Figure 6. Effect of ampicillin concentration loaded on the nanocomposite on antibacterial activity. *Staphylococcus aureus* was cultivated in Nutrient Broth, pH=7.0; at 37^{0}C for 48h, and shaking with 120 rpm; values in the figure are mean of triplicates ± SE, $p<0.05$).

Consistent with encapsulation efficiency, the antibacterial inhibition of M100+Amp (≈87%) was lower than that of free ampicillin (≈92%) at 7.5 μg/mL. In contrast, C100+Amp and C3M1+Amp achieved inhibition rates of approximately 93.5%. Considering the encapsulation efficiency (70–80%), the minimum inhibitory concentration (MIC) of ampicillin-loaded chitosan/cellulose nanocomposites against *S. aureus* was reduced to 3.0–4.0 μg/mL, comparable to or lower than values reported for other nano-delivery systems [34,35].

3.2.2. Time-Dependent Antibacterial Performance and Anti-Resistance Effect

Time-kill studies against *S. aureus* revealed distinct release and activity profiles between free ampicillin and nanocomposite-loaded formulations. During the initial 3 h, free ampicillin showed slightly higher antibacterial activity (≈45%) than nanocomposites (≈40–44%), reflecting the delayed release of encapsulated drug. However, after 6 h, nanocomposite formulations exhibited superior antibacterial effects (≈64–65%) compared with free ampicillin (≈63%), indicating sustained drug release.

At 12 h, all formulations reached maximal inhibition (≈92–93%), except for M100+Amp, which showed significantly lower activity (≈87%). Notably, prolonged incubation up to 48 h revealed a gradual decline in the antibacterial efficacy of free ampicillin, confirming the intrinsic resistance of the *S. aureus* strain. In contrast, chitosan/carboxymethyl cellulose nanocomposites, particularly C3M1+Amp and C1M1+Amp, maintained stable antibacterial activity over 48 h, demonstrating an enhanced ability to counteract antibiotic resistance. These results indicate that ampicillin encapsulated in chitosan/carboxymethyl cellulose nanocomposites, characterized by higher encapsulation efficiency (EE%), as well as a slower and more sustained release profile, exhibited significantly enhanced antibacterial activity compared with previously reported systems [21,22,34–36].

 doi:10.20944/preprints202512.2817.v1

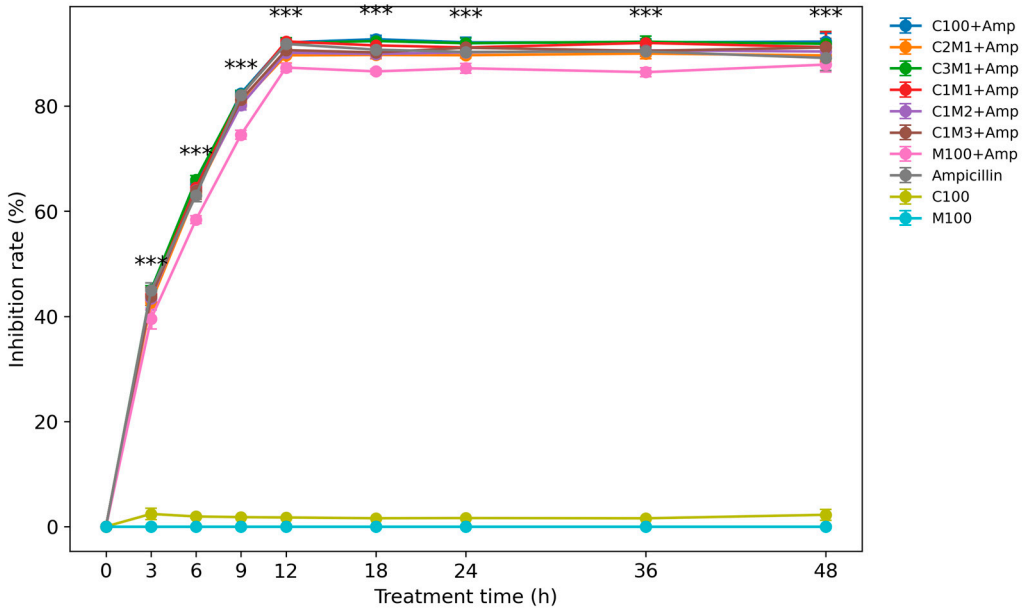

Figure 7. Efectiveness of chitosan/carboxymethyl cellulose loaded Ampicillin Loading on *S. aureus* Antibacterial Activity. *Staphylococcus aureus* was cultivated in Nutrient Broth, pH=7.0; at 37^{0}C for 48h, and shaking with 120 rpm; values in the figure are mean of triplicates ± SE, p<0.01).

3.2.3. MIC and MBC Evaluation

The MIC and minimum bactericidal concentration (MBC) values of ampicillin-loaded chitosan/cellulose nanocomposites are summarized in Table 2. The MIC and MBC values ranged from 3.20–3.47 μg/mL and 5.33–5.80 μg/mL, respectively, which are significantly lower than those of free ampicillin (4.23 and 6.80 μg/mL), C100+Amp, and M100+Amp. Moreover, the MBC/MIC ratios of chitosan/cellulose nanocomposites (1.66–1.70) were lower than those of chitosan nanoparticles and carboxymethyl cellulose loaded ampicillin, indicating improved bactericidal efficiency.

Table 2. MIC and MBC of chitosan/carboxymethyl cellulose nanocomposite loaded ampicillin on *Staphyllococcus aureus.*

No.	Samples	MIC (μg/mL)	MBC (μg/mL)	MBC/MIC ratio
1	C100 + Amp	3.53^{c} ± 0.12	6.47^{c} ± 0.12	1.83
2	C2M1 + Amp	3.20^{a} ± 0.00	5.33^{a} ± 0.12	1.66
3	C1M1 + Amp	3.30^{ab} ± 0.12	5.73^{b} ± 0.12	1.70
4	C1M2 + Amp	3.47^{c} ± 0.12	5.80^{b} ± 0.00	1.67
5	M100 + Amp	4.27^{d} ± 0.12	7.07^{e} ± 0.12	1.65
6	Ampicillin (Amp)	4.23^{d} ± 0.12	6.80^{d} ± 0.00	1.60

Values are presented as mean ± standard deviation (n = 3). Different superscript letters (a–d) within the same column indicate statistically significant differences (p < 0.05).

This study demonstrates that spray-dried chitosan/carboxymethyl cellulose (CMC) nanocomposites constitute an efficient antibiotic delivery system with enhanced physicochemical and antibacterial performance.

First, the formation of stable polyelectrolyte nanocomposites was achieved through electrostatic complexation between cationic chitosan and anionic CMC. Similar polyelectrolyte interactions have been reported to improve particle stability and functional performance in polysaccharide-based nanocarriers [37–41]. However, most previous systems relied on chemical crosslinkers or ionic gelation agents such as tripolyphosphate (TPP), which may limit scalability and biocompatibility [16,25].

 doi:10.20944/preprints202512.2817.v1

Second, the nanocomposites exhibited exceptionally high positive zeta potentials (+70 to +90 mV) at optimal chitosan/CMC ratios. These values are significantly higher than those commonly reported for chitosan nanoparticles prepared by ionic gelation or spray drying (+20 to +55 mV). Recent studies have highlighted that increased surface charge enhances colloidal stability and bacterial membrane interaction, thereby improving antimicrobial efficacy [16,19,25].

Third, ampicillin encapsulation efficiency reached approximately **80–82%,** exceeding values reported for chitosan-only or chitosan/starch systems (typically 60–75%) [21,22]. This improvement is attributed to the dense ionic network formed between oppositely charged polymers, which has been shown to enhance drug retention and loading capacity in polyelectrolyte-based carriers.

Fourth, ampicillin-loaded chitosan/CMC nanocomposites showed sustained and enhanced antibacterial activity against *Staphylococcus aureus*, maintaining inhibitory efficacy for up to 48 h. In contrast, free ampicillin exhibited a time-dependent decrease in activity, consistent with the reported resistance profile of *S. aureus* strains [21,26]. Similar sustained antibacterial effects have been observed in nano-enabled antibiotic delivery systems that protect β-lactam antibiotics from enzymatic degradation and efflux mechanisms [3,5,13,26,27,31].

Finally, the significantly reduced MIC and MBC values of the nanocomposites compared with free ampicillin and control nanoparticles confirm improved bacteriostatic and bactericidal performance. Previous studies have demonstrated that nano-encapsulation can lower MIC values by enhancing local drug concentration at the bacterial surface and disrupting cell membrane integrity [34–36].

4. Conclusions

Electrolyte gelation combined with spray drying provides a robust and efficient strategy for fabricating chitosan/carboxymethyl cellulose nano-microcomposites as antibiotic delivery carriers. The synergistic interaction between chitosan and CMC facilitated the formation of stable nanocomposites exhibiting a high surface charge, superior ampicillin encapsulation efficiency, and sustained antibacterial activity against *Staphylococcus aureus*. The markedly reduced MIC and MBC values, together with prolonged antibacterial effectiveness, clearly demonstrate the ability of this delivery system to enhance antibiotic performance and potentially mitigate bacterial resistance.

Overall, these findings highlight chitosan/carboxymethyl cellulose nano-microcomposites as a promising, safe, and cost-effective platform for antimicrobial applications, providing a solid foundation for further preclinical evaluation and translational development in drug delivery and infection control.

Author Contributions: Conceptualization, A.-D.N and S-L-W; methodology, A.-D.N; software, A.-D.N and V.-B.N; validation, S-L-W and A.-D.N; formal analysis, V.-B.N, D.-S.N; H.-H.D; T.-H.N; V.-H.T; S-L-W and A.-D.N; investigation, V.-N.N and T.-H.N; resources, A.-D.N; data curation, A.-D.N and S-L-W; writing—original draft preparation, A.-D.N; writing—review and editing, V.-B.N, A.-D.N and S-L-W; supervision, A.-D.N.All authors have read and agreed to the published version of the manuscript.

Funding: No.

Institutional Review Board Statement: Not applicable.

Data Availability Statement: Suggested Data Availability Statements are available in section “MDPI Research Data Policies” at https://www.mdpi.com/ethics.

Conflicts of Interest: The authors declare no conflicts of interest.

References

1. Stefanache, A.; Lungu, I.I.; Anton, N.; Damir, D.; Gutu, C.; Olaru, I.; Plesea Condratovici, A.; Duceac, M.; Constantin, M.; Calin, G.; et al. Chitosan Nanoparticle-Based Drug Delivery Systems: Advances, Challenges, and Future Perspectives. *Polymers* **2025**, *17*, 1453. https://doi.org/10.3390/polym17111453

 doi:10.20944/preprints202512.2817.v1

2. Biswas, R.; Mondal, S.; Ansari, M.A.; Sarkar, T.; Condiuc, I.P.; Trifas, G.; Atanase, L.I. Chitosan and Its Derivatives as Nanocarriers for Drug Delivery. *Molecules* **2025**, *30*, 1297. https://doi.org/10.3390/molecules30061297
3. Farhangi, M.; Kobarfard, F.; Mahboubi, A.; Vatanara, A.; Mortazavi, A.S. Preparation of an Optimized Ciprofloxacin-Loaded Chitosan Nanomicelle with Enhanced Antibacterial Activity. *Drug Dev. Ind. Pharm.* **2018**, *44*, 1–10. https://doi.org/10.1080/03639045.2018.1442847
4. Ssekatawa, K.; Byarugaba, D.K.; Kato, C.D.; Ejobi, F.; Tweyongyere, R.; Lubwama, M.; Kirabira, J.B.; Wampande, E.M. Nanotechnological Solutions for Controlling Transmission and Emergence of Antimicrobial-Resistant Bacteria: Future Prospects and Challenges. *J. Nanopart. Res.* **2020**, *22*, 117. https://doi.org/10.1007/s11051-020-04810-6
5. Abdel-Hakeem, M.A.; Maksoud, A.I.A.; Aladhadh, M.A.; Almuryif, K.A.; Elsanhoty, R.M.; Elebeedy, D. Gentamicin–Ascorbic Acid Encapsulated in Chitosan Nanoparticles Improved in Vitro Antimicrobial Activity and Minimized Cytotoxicity. *Antibiotics* **2022**, *11*, 1530. https://doi.org/10.3390/antibiotics11111530
6. Abdelmalek, I.; Svahn, I.; Mesli, S.; Simonneaux, G.; Mesli, A. Formulation, Evaluation and Microbiological Activity of Ampicillin and Amoxicillin Microspheres. *J. Mater. Environ. Sci.* **2014**, *5*, 1799–1807.
7. Alarfaj, A.A. Preparation, Characterization and Antibacterial Effect of Chitosan Nanoparticles against Food Spoilage Bacteria. *J. Pure Appl. Microbiol.* **2019**, *13*, 1273–1278. https://doi.org/10.22207/JPAM.13.2.64
8. Alwaan, I.M.; Ahmed, M.; Al-Kelaby, K.K.A.; Allebban, Z.S.M. Starch–Chitosan Modified Blend as Long-Term Controlled Drug Release for Cancer Therapy. *Pak. J. Biotechnol.* **2018**, *15*, 947–955.
9. Yanat, M.; Schoen, K. Preparation Methods and Applications of Chitosan Nanoparticles with an Outlook toward Reinforcement of Biodegradable Packaging. *React. Funct. Polym.* **2021**, *161*, 104849. https://doi.org/10.1016/j.reactfunctpolym.2021.104849
10. Ehyaeirad, N.; Babolanimogadam, N.; Dadkhah, M.; Shirmard, L.R. Polylactic Acid Films Incorporated with Nanochitosan, Nanocellulose, and Ajwain Essential Oil. *Carbohydr. Polym. Technol. Appl.* **2024**, *7*, 100425.
11. Fotie, G.; Limbo, S.; Piergiovanni, L. Manufacturing of Food Packaging Based on Nanocellulose: Current Advances and Challenges. *Nanomaterials* **2020**, *10*, 1726. https://doi.org/10.3390/nano10091726
12. Gonzalez, A.; Ferrante, M.; Gende, L.; Alvarez, V.A.; Gonzalez, J.S. Polyelectrolyte Complex-Based Chitosan/Carboxymethylcellulose Powdered Microgels Loaded with Eco-Friendly Silver Nanoparticles. *Polysaccharides* **2025**, *6*, 84. https://doi.org/10.3390/polysaccharides6030084
13. Ibrahim, H.M.; El-Bisi, M.K.; Taha, G.M.; El-Alfy, E.A. Preparation of Biocompatible Chitosan Nanoparticles Loaded with Antibiotics. *Int. J. Biol. Macromol.* **2020**, *161*, 1247–1260. https://doi.org/10.1016/j.ijbiomac.2020.06.206
14. Sobhani, Z.; Samani, S.M.; Montaseri, H.; Khezri, E. Nanoparticles of Chitosan Loaded with Ciprofloxacin: Fabrication and Antimicrobial Activity. *Adv. Pharm. Bull.* **2017**, *7*, 427–432.
15. Sohail, R.; Abbas, S.R. Evaluation of Amygdalin-Loaded Alginate–Chitosan Nanoparticles. *Int. J. Biol. Macromol.* **2020**, *153*, 36–45.
16. Nguyen, V.T.; Nguyen, T.T.H.; Wang, S.L.; Vo, T.T.H.; Nguyen, A.D. Preparation of Chitosan Nanoparticles by TPP Ionic Gelation Combined with Spray Drying. *Res. Chem. Intermed.* **2017**, *43*, 3527–3537.
17. Schumacher, I.; Margalit, R. Liposome-Encapsulated Ampicillin. *J. Pharm. Sci.* **1997**, *86*, 635–641.
18. Asadpoor, M.; Varasteh, S.; Pieters, R.J.; Folkerts, G.; Braber, S. Differential Effects of Oligosaccharides on Ampicillin Activity. *PharmaNutrition* **2021**, *16*, 100264.
19. La, T.K.N.; Phung, M.L.; Wang, S.L.; Nguyen, A.D. Preparation of Chitosan Nanoparticles by Spray Drying. *Res. Chem. Intermed.* **2014**, *40*, 2165–2175.
20. Oudih, S.B.; Tahtat, D.; Khodja, A.N.; Mahlous, M.; Hammache, Y.; Guittoum, A.E.; Gana, S.K. Chitosan Nanoparticles with Controlled Size and Zeta Potential. *Polym. Eng. Sci.* **2023**, *63*, 2011–2021.
21. Nguyen, V.N.; Tran, M.D.; Doan, M.D.; Nguyen, D.S.; Nguyen, T.H.; Doan, C.T.; Wang, S.L.; Nguyen, A.D. Enhancing the Antibacterial Activity of Ampicillin-Loaded Chitosan/Starch Nanocomposites. *Carbohydr. Res.* **2024**, *545*, 109274.

 doi:10.20944/preprints202512.2817.v1

22. Nguyen, V.N.; Doan, M.D.; Nguyen, T.H.; Wang, S.L.; Nguyen, A.D. Preparation and Characterization of Chitosan/Starch Nanocomposites Loaded with Ampicillin. *Polymers* **2024**, *16*, 2647.
23. Ha, N.M.C.; Nguyen, T.H.; Wang, S.L.; Nguyen, A.D. Preparation of NPK Nanofertilizer Based on Chitosan Nanoparticles. *Res. Chem. Intermed.* **2019**, *45*, 51–63.
24. Dudhani, A.R.; Kosaraju, S.L. Bioadhesive Chitosan Nanoparticles. *Carbohydr. Polym.* **2010**, *81*, 243–251.
25. Kašpar, O.; Jakubec, M.; Štěpánek, F. Characterization of Spray-Dried Chitosan–TPP Microparticles. *Powder Technol.* **2013**, *240*, 31–40.
26. Murei, A.; Ayinde, W.B.; Gitari, M.W.; Samie, A. Functionalization and Antimicrobial Evaluation of Antibiotics with Silver Nanoparticles. *Sci. Rep.* **2020**, *10*, 11596.
27. Nairi, V.; Medda, L.; Monduzzi, M.; Salis, A. Adsorption and Release of Ampicillin from Mesoporous Silica. *J. Colloid Interface Sci.* **2017**, *497*, 217–225.
28. Hong, T.; Yin, J.Y.; Nie, S.P.; Xie, M.Y. Applications of Infrared Spectroscopy in Polysaccharide Structural Analysis. *Food Chem. X* **2021**, *12*, 100168.
29. Lustriane, C.; Dwivany, F.M.; Suendo, V.; Reza, M. Effect of Chitosan and Chitosan Nanoparticles on Banana Fruits. *J. Plant Biotechnol.* **2018**, *45*, 36–44.
30. Hussein-Al-Ali, S.H.; El Zowalaty, M.E.; Hussein, M.Z.; Geilich, B.M.; Webster, T.J. Ampicillin-Conjugated Magnetic Nanoantibiotic. *Int. J. Nanomedicine* **2014**, *9*, 3801–3814.
31. Ibrahim, H.M.; El-Bisi, M.K.; Taha, G.M.; El-Alfy, E.A. Chitosan Nanoparticles Loaded Antibiotics. *J. Appl. Pharm. Sci.* **2015**, *5*, 85–90.
32. World Health Organization (WHO). High Levels of Antibiotic Resistance Found Worldwide. WHO News Release, 2018.
33. Fan, P.; Ma, Z.; Partow, A.J.; Kim, M.; Grace, M.; Shoemaker, G.M.; Tan, R.; Tong, Z.; Nelson, C.D.; Jang, Y.; Jeong, K.C. A Novel Combination Therapy Using Chitosan Nanoparticles. *Int. J. Biol. Macromol.* **2022**, *195*, 506–514.
34. Anal, A.K.; Stevens, W.F.; Remuñán-López, C. Ionotropically Cross-Linked Chitosan Microspheres. *Int. J. Pharm.* **2006**, *312*, 166–173.
35. Foxley, M.A.; Friedline, A.W.; Jensen, J.M.; Nimmo, S.L.; Scull, E.M.; Strange, S.; Xiao, M.T.; Smith, B.E.; King, J.B.; Rice, C.V. Efficacy of Ampicillin against MRSA. *J. Antibiot.* **2016**, *69*, 871–878.
36. Godoy, C.A.; Balic, I.; Moreno, A.A.; Diaz, O.; Arenas Colarte, C.; Bruna Larenas, T.; Gamboa, A.; Caro Fuentes, N. Antimicrobial Activity of Chitosan Nanoparticles. *Pharmaceutics* **2025**, *17*, 186. https://doi.org/10.3390/pharmaceutics17020186
37. Aranaz, I.; Alcántara, A.R.; Civera, M.C.; Arias, C.; Elorza, B.; Heras Caballero, A.; Acosta, N. Chitosan: An Overview. *Polymers* **2021**, *13*, 3256.
38. Dash, M.; Chiellini, F.; Ottenbrite, R.M.; Chiellini, E. Chitosan in Biomedical Applications. *Prog. Polym. Sci.* **2011**, *36*, 981–1014.
39. Ahmed, T.A.; Aljaeid, B.M. Chitosan-Based Drug Delivery Systems. *Drug Des. Devel. Ther.* **2016**, *10*, 483–507.
40. Ferreira, D.C.M.; Ferreira, S.O.; de Alvarenga, E.S.; de Fátima Ferreira Soares, N.; Coimbra, J.S.S.; de Oliveira, E.B. Polyelectrolyte Complexes of Chitosan and CMC. *Carbohydr. Polym. Technol. Appl.* **2022**, *3*, 100197.
41. Le, H.; Karakasyan, C.; Jouenne, T.; Le Cerf, D.; Dé, E. Polymeric Nanocarriers for Antibiotic Delivery. *Appl. Sci.* **2021**, *11*, 10695.